World J Microbiol Biotechnol (2017) 33:146
DOI 10.1007/s11274-017-2310-x

ORIGINAL PAPER

Site-directed mutagenesis under the direction of in silico protein docking modeling reveals the active site residues of 3-ketosteroid-Δ^1-dehydrogenase from *Mycobacterium neoaurum*

Ning Qin[1] · Yanbing Shen[1] · Xu Yang[1] · Liqiu Su[1] · Rui Tang[1] · Wei Li[1] · Min Wang[1]

Received: 19 November 2016 / Accepted: 10 June 2017 / Published online: 20 June 2017

Abstract 3-Ketosteroid-Δ^1-dehydrogenases (*KsdD*) from *Mycobacterium neoaurum* could transform androst-4-ene-3,17-dione (AD) to androst-1,4-diene-3,17-dione. This reaction has a significant effect on the product of pharmaceutical steroid. The crystal structure and active site residues information of *KsdD* from *Mycobacterium* is not yet available, which result in the engineering of *KsdD* is tedious. In this study, by the way of protein modeling and site-directed mutagenesis, we find that, Y122, Y125, S138, E140 and Y541 from the FAD-binding domain and Y365 from the catalytic domain play a key role in this transformation. Compared with the wild type, the decline in AD conversion for mutants illustrated that Y125, Y365, and Y541 were essential to the function of *KsdD*. Y122, S138 and E140 contributed to the catalysis of *KsdD*. The following analysis revealed the catalysis mechanism of these mutations in *KsdD* of *Mycobacterium*. These information presented here facilitate the manipulation of the catalytic properties of the enzyme to improve its application in the pharmaceutical steroid industry.

Keywords *Mycobacterium neoaurum* · 3-Ketosteroid-Δ^1-dehydrogenase · Androst-4-ene-3,17-dione · Site-directed mutagenesis · Biotransformation

Introduction

Androst-4-ene-3,17-dione (AD) is an important precursor in the synthesis of pharmaceutical steroid, and it can be used to synthesize almost all kinds of steroidal medication (YuKimatsu and Kaji 1979). *Mycobacterium neoaurum* is the species that is protected by numerous patents to obtain AD from the side-chain cleavage of phytosterol (PS) (Fernandes et al. 2003; Szentirmai 1990; Wovcha et al. 1979). However, the production of AD is often associated with androst-1,4-diene-3,17-dione (ADD). Thus, separating these substances in downstream processing is difficult because of their high structural similarity, which reduces product yield and affects product quality (Malaviya and Gomes 2008; Wei et al. 2010; Zhang et al. 2013).

Current research has shown that it is 3-ketosteroid-Δ^1-dehydrogenase (*KsdD*) that change AD into ADD by introducing a double bond into the C1–C2 position of the 3-ketosteroid A-ring. Several strains of bacteria (Donova 2007), such as *Arthrobacter* sp. (Fokina et al. 1997), *Pseudomonas* sp. (Adham et al. 2003; Plesiat et al. 1991), *Rhodococcus* (Geize et al. 2000, 2001) and *Mycobacterium* (Wei et al. 2010) exhibit $C_{1,2}$ dehydrogenation. For the significant industrial applications, *KsdD* from *Mycobacterium* has long attracted wide attention, but the studies mostly focused on mutation breeding by physical and chemical methods (Marsheck et al. 1972; Zhong et al. 2009), exploring novel enzyme by bioinformation analysis (Bragin et al. 2013; Geize et al. 2007; Shtratnikova et al. 2014; Zhang et al. 2015) and engineering of *Mycobacterium* by

Electronic supplementary material The online version of this article (doi:10.1007/s11274-017-2310-x) contains supplementary material, which is available to authorized users.

✉ Yanbing Shen
shenyb@tust.edu.cn

✉ Min Wang
minw@tust.edu.cn

[1] Key Laboratory of Industrial Fermentation Microbiology, Ministry of Education, College of Biotechnology, Tianjin University of Science & Technology, Tianjin 300457, People's Republic of China

molecular approaches (Wei et al. 2010), the study on the structure and active sites residues of *KsdD* from *Mycobacterium* is tedious.

The crystal structure of the *KsdD* enzymes of *Mycobacterium* is not yet available. Studies about the structure and active sites of *KsdD* mostly focused on the *KsdD* from *Rhodococcus* (Fujii et al. 1999; Geize et al. 2002; Matsushita and Itagaki 1992). Oosterwijk et al. (2012) reported the first crystal structure of KsdD4 from *Rhodococcus jostii* RHA1. Rohman et al. (2012, 2013) reported the crystallization and X-ray crystallographic analysis of *KsdD* from *Rhodococcus erythropolis* SQ1. These paper suggested that, different from elimination (E2) mechanism, the enzyme catalyzed dehydrogenation more likely follows a stepwise unimolecular elimination conjugate base (E1cB) mechanism, in which departure of the first hydrogen atom precedes that of the second hydrogen accompanied by the formation of an intermediate. During this progress, Y487 and G491 act as an electrophile to promote labilization of the C2 hydrogen atoms of 3-ketosteroid substrate. Meanwhile, Y318, which is assisted by Y119, as a general base abstract a proton from the C2 atom and result in either an enolate or a carbanionic intermediate; subsequently, a double bond between the C1 and C2 atoms is formed.

Sructural and active sites information on *KsdD* from *Mycobacterium* is still limited, which restricts the progress of structure-based engineering of *KsdD*. Meanwhile, the variation of active sites of *KsdD* from *Mycobacterium* have significant impact in the production of AD. Liu et al. (2015) revealed the mutant *KsdD* gene resulted in the change of AD/ADD molar ratios. Shao et al. (2016) reported that Val366 of KsdDI (from *M. neoaurum* ST-095) changed to Ser366 of KsdDII (from *M. neoaurum* JC-12) affected *KsdD* activity (Zhong et al. 2009). Bragin et al. (2013) and Shtratnikova et al. (2014) sequenced the full genome of *Mycobacterium* spp. VKM Ac-1815D and 1816D and pointed out that one of single nucleotide polymorphisms (SNPs), located in a single-copy *ksdD* gene, caused the major practical difference between VKM Ac-1815D and 1816D: production of AD and ADD, respectively, as major products from sterols (Marsheck et al. 1972).

In our previous report, Shen et al. (2012) found that *M. neoaurum* TCCC 11028 (*MNR*) and its derived mutant strain *M. neoaurum* TCCC 11028 M3 (*MNR* M3) significantly differ in the ADD/AD ratio, with 44.5:1 and 1:8.3, respectively. The change of S138 in *KsdD-MNR* to L138 in *KsdD-MNR* M3 because of C413T in the *KsdD* gene, significantly affected its activity (Xie et al. 2015).

Given the significance of the sites of *KsdD* from *Mycobacterium* in the production of AD and to have a direction in the engineering of *KsdD* from *Mycobacterium*, we focused on the structure and active site residues of *KsdD* from *Mycobacterium*.

In the present study, we aimed to obtain the structure information of the active sites of *KsdD* enzymes from *Mycobacterium*. Thus, mutant genes *KsdD* Y125F, Y365F, Y541F, Y122F, S138A, E140V, and Y472F were constructed based on in silico protein docking modeling using site-directed mutagenesis and exogenous expression. Biotransformation experiments were also performed. Changes in the enzyme activity of mutants were determined by the difference of the conversion rate. The structural mechanism of mutations in *KsdD* of *Mycobacterium* was analyzed based on this process. The information presented facilitate the manipulation of the catalytic properties of the enzyme to improve its application in the pharmaceutical steroid industry.

Materials and methods

Chemicals

AD and ADD were obtained from Sigma-Aldrich Co. (USA). All of the utilized chemical solvents and salts were of analytical grade or higher.

Bacterial strains and culture conditions

Mycobacterium neoaurum TCCC 11028 (*MNR*) used in this study was obtained from Tianjin University of Science and Technology Culture Collection Center (TCCC), Tianjin, China. The methods of microbial cultivation and bioconversion were established by Shen et al. (2012). *Escherichia coli* DH5α and *E. coli* BL21 (DE3), which express wild-type *KsdD* and *KsdD* with mutated amino acids, were grown at 37 °C overnight in LB medium containing 50 μg/mL ampicillin and shaken at 180 rpm. This 5 mL pre-culture was seeded by 1–100 in 800 mL of fresh LB medium with 25 μg/mL ampicillin. The culture was grown at 37 °C and shaken at 200 rpm. When optical density at 600 nm reached 0.8, 100 mM isopropyl-β-D-thiogalactopyranoside was added to trigger the expression of *KsdD*. *E. coli* cells were grown in 3 L flasks at 16 °C for 18 h, with shaking at 200 rpm. The cultures were centrifuged at 5000×*g* for 10 min. The cell pellets were washed three times with 20 mM PBS buffer (100 mM dipotassium hydrogen phosphate-potassium dihydrogen phosphate, 1% glycerol, pH 7.3) and resuspended in the same buffer to an optical density of 10 at 600 nm using a Shimadzu model UV-1601PC spectrophotometer (Kyoto, Japan).

In silico generation of protein structure and molecular structures

For the reason of *KsdD* from *R. erythropolis* SQ1 shared 40.83% sequence identity and 42.60% sequence similarity to *KsdD* from *MNR* (sequence coverage is 98%), the crystal structure of *KsdD* from *R. erythropolis* SQ1 could be used as the template in the homologous modeling. Based on the known crystal structure of *KsdD* from *R. erythropolis* SQ1 (PDB:4C3Y, 2.3 Å resolution), the 3D structure of *KsdD* from *MNR* was homologically modeled using MODeller 9.15 program (http://salilab.org/modeller/). The 3D structural information of AD, which was used as the ligand, was handled using Sybyl2.0 program.

Docking studies

To understand the binding model of compound AD with *KsdD*, compound AD was docked into the active site by Sybyl2.0 program. The molecular construction and energy minimization of compound AD was prepared by Sybyl2.0 program. Based on the conformation of *KsdD* docking with AD, all amino acids in the substrate-binding groove of *KsdD* and in proximity to AD within 5 Å were located by PyMol software (http://pymol.org/). Swiss-model (http://swissmodel.expasy.org/) was used to simulate the conformation of the site mutants.

Construction of the mutant *KsdD* genes and expression of *KsdD*

KsdD gene were codon-optimized for expression in *E. coli* and synthesized by BGI-Shenzhen. To amplify *KsdD*, forward primer *KsdD* exp-F (5′-GGAATTCCATATG GTGTTTTATATGACCGCGCAGG-3′) was design, including start codon, *Nde* I restriction site (underlined), and reverse primer *KsdD* exp-R (5′-CGGGATCCGAC GCTTTGCCCGCTAAATGTA-3′) with removed stop codon and included a *Bam*H I restriction site (underlined). PCR product *KsdD* (1701 bp) was cloned into *Nde* I/*Bam*H I-digested pET-22b(+) to introduce a C-terminal His tag into this protein. The resulting construct pET-22b(+)-*KsdD* was transformed into *E. coli* BL21 (DE3). Mutagenesis was constructed by overlap PCR. Two-step PCR was essential to introduce a single amino acid mutation. For each mutation, a new pair of mutagenic primer was designed according to the nucleotide sequence of *KsdD* (Table 1). The mutated nucleotides are shown as capital letters. Reverse mutagenic primer sequences were complementary to the forward primers and had the same lengths. First, the mutagenic primers were compared with outside primers to introduce base mutation. A pair of DNA fragment, in which one side overlapped with the other, was amplified. Mutation was then introduced into the overlapped region. After purification, the PCR product was used as the template to amplify the total *KsdD* using outside primers.

Table 1 primers used in this study

Primers	Nucleotide sequence (5′–3′)
122-R1	gataataatcgctaAagcccggcacccaac
122-F2	gttgggtgccgggctTtagcgattattat
125-R1	tccggataaAaatcgctatagccc
125-F2	tatagcgattTttatccggaaacccc
138-R1	tttcggttcaacgGCacgaccggtcgctt
138-F2	agcgaccggtcgtGCcgttgaaccgaaa
140-R1	aaacggtttcggtAcaacgctacgaccggt
140-F2	accggtcgtagcgttgTaccgaaaccgtt
365-R1	ttccacaAacggcatgctttcg
365-F2	atgccgtTtgtggaagcgtgc
472-R1	tcggatcgccataaAagcgatcatacgcgct
472-F2	agcgcgtatgatcgctTttatggcgatccg
541-R1	ggaccaggaAaggtatgacccatcac
541-F2	gtcatacctTtcctggtccgggc

PCR product–whole *KsdD* (1701 bp) was inserted into *Nde* I/*Bam*H I-digested pET-22b(+), followed by the transformation of ligation product into *E. coli* DH5α. Individual clones of these *E. coli* variants were grown, and their plasmids were isolated to identify the result of the clones digested by *Nde* I/*Bam*H I. After confirmation through DNA sequencing, the recombinant vector was transformed into *E. coli* BL21 (DE3) for exogenous protein expression.

Biotransformation reactions

The resuspension was incubated with AD at a final concentration of 1.2 g/L at 20 °C with shaking at 200 rpm. The samples were withdrawn at various time intervals and extracted with the same volume of ethyl acetate. The organic phases were collected and detected through thin layer chromatography (TLC) and HPLC. Wild *E. coli* BL21 (DE3)/pET-22b(+)-*KsdD* was used as negative control. The transformation products detected by TLC and HPLC were prepared and analyzed following the procedures described by Shen et al. (2012). Solid extracts which was dried in vacuum from organic phases, were redissolved in the HPLC mobile phase and filtered through a 0.22 μm filter before HPLC analysis. HPLC analysis was performed on a Kromasil C18 column (250×4.6 mm) with methanol/water (4:1, v/v) as mobile phase at 30 °C with UV absorbance detection at 254 nm. The concentrations of AD and ADD were determined from the calibration curves of eluent solutions of standard AD and ADD.

Results

In silico design of mutant *KsdD*

KsdD is a FAD dependent enzyme. The putative N-terminal FAD-binding motifs in the *KsdD* was consistent with the sequence as previously described (Geize et al. 2000; Wei et al. 2010; Rohman et al. 2013) GSG(A/G)(A/G)(A/G)X17E (Fig. S1). During the homological modelling, FAD in 4c3y was reserved. As shown in Fig. S3, this model was accepted and can be used for the following research.

As shown in Fig. 1, *KsdD* can be divided into FAD-binding domain and catalytic domain. FAD was bound in the pocket and the isoalloxazine ring pointed to catalytic domain. AD was in the middle of catalytic domain and FAD-binding domain. Figure 2 showed that carbonyl of C3 sterone's was in the hydrogen bonding distance with Y365, Y541, and G545 of *KsdD* from *MNR*, similar to the corresponding amino acid residues Y318, Y487, and G491 in the active center of *KsdD* from *R. erythropolis* SQ1 (Rohman et al. 2013). The change of the ligand from ADD in 4c3y to AD in docking removed the H bond between the N5 atom of the isoalloxazine ring of FAD with C1 atom of A ring of AD. However, the isoalloxazine ring of FAD was still closed to the A ring of AD, which was essential for the transfer of α-hydrogen of the C1 atom of A ring as a hydride ion.

Based on the docked conformation of *KsdD* and AD, 27 residues of *KsdD* in proximity to AD within 5 Å were located using PyMol software (Fig. 2). According to the results of Rohman et al. (2013), who recognized the necessity of the general base in the catalysis of *KsdD*, seven potential mutation sites, namely, Y122, Y125, S138, E140

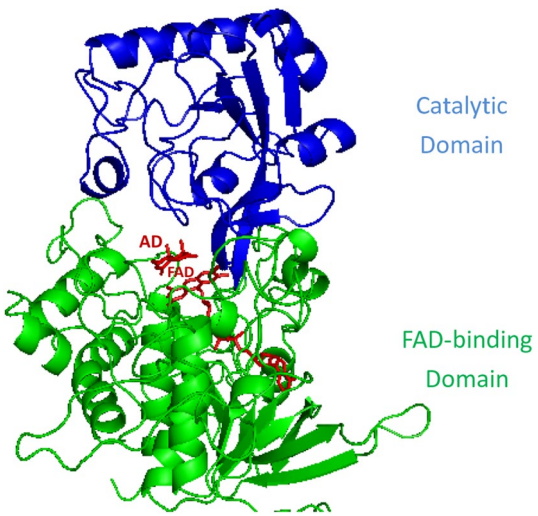

Fig. 1 The model of *KsdD* with AD and FAD. *KsdD* can be divided into FAD-binding domain (*green*) and catalytic domain (*blue*)

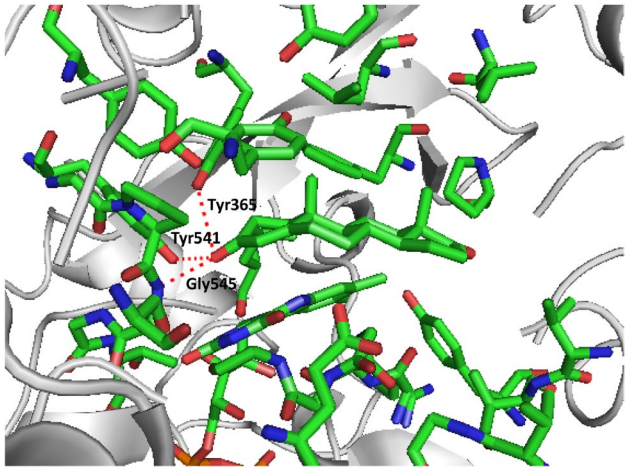

Fig. 2 Local model of the residues of *KsdD* around AD within 5 Å

and Y541 from the FAD-binding domain and Y365 and Y472 from the catalytic domain, were determined. G545 from the FAD-binding domain was ignored because it was a backbone amide in the hydrogen bonding distance of the C3 carbonyl group. An amino acid sequence alignment of the available *KsdD*s from different bacteria revealed that, among these amino acids at the active site of *KsdD*, Y125, Y541, G545 and Y365 from the catalytic domain were strictly conserved (Fig. S1). As shown in the phylogenetic tree (Fig. S2) which all *KsdD* proteins were majorly clustered into some branches, Y122, S138, E140 and Y472 were conserved (Fig. S1) in the branch of *MNR*.

Interestingly, S138 of the *KsdD* of *MNR*, which spontaneously mutated to L138 of the *KsdD* of *MNR* M3 and triggered the decline in activity of *KsdD* (Xie et al. 2015), was also included. This finding implied that 5 Å was appropriate. Sites located at an appropriate distance to the ligand may promote keto-enol tautomerization and labilization of C2 hydrogen atoms.

Construction of the mutations

As shown by SDS–PAGE analysis in Fig. 3a, *KsdD* was successfully expressed by increased yield in the host with the expected molecular weight of 63.4 kDa, which was similar to the report of Shao et al. (2016). This protein was also identified by mass spectrometry. Overlap PCR was used to implement the point mutations. After mutagenesis, through the same process of the wild *KsdD*, the mutations were constructed and identified using the result of clones that were digested by *Nde* I/*Bam*H I before sequencing. SDS–PAGE analysis revealed that (Fig. 3b) Y122F, Y125F, S138A, E140V, Y365F, Y472F, and Y541F were expressed as well. Gray level difference analysis of protein bands

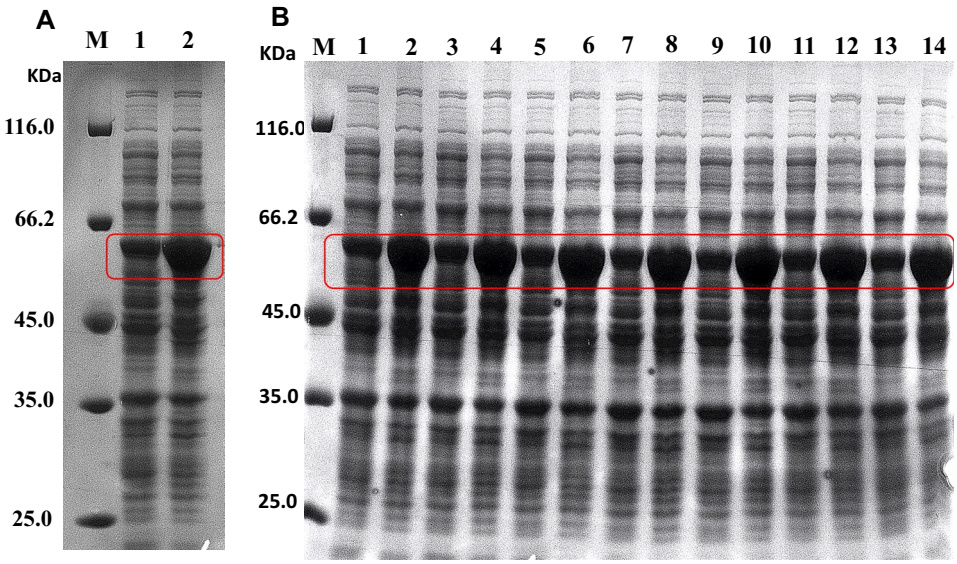

Fig. 3 Heterologous expression of *KsdD* and mutations in *E. coli*. **a** SDS–PAGE analysis of *E. coli* BL21 (DE3)/pET-22b(+)-*KsdD-MNR Lane 1 E. coli* BL21 (DE3)/pET-22b(+)-*KsdD-MNR* (before codon optimization); *lane 2 E. coli* BL21 (DE3)/pET-22b(+)-*KsdD-MNR* (after codon optimization). **b** SDS–PAGE analysis of mutations of *KsdD* in *E. coli. Lane 1* Y122F; *lane 2* Y122F induced; *lane 3* Y125F; *lane 4* Y125F induced; *lane 5* S138A; *lane 6* S138A induced; *lane 7* E140V; *lane 8* E140V induced; *lane 9* Y365F; *lane 10* Y365F induced; *lane 11* Y472F; *lane 12* Y472F induced; *lane 13* Y541F; *lane 14* Y541F induced

implied that no significant changes in *KsdD* expression were caused by the mutations.

Effect of amino acid mutations on *KsdD* activity

Under the same conditions, wild *KsdD* and mutant *KsdD* were used to transform AD to ADD. The results of TLC (Fig. 4a) showed the different activities of *KsdD* in wild type and mutant. The conversion rate of AD by wild type was nearly 50%, and mutant strains could be divided into two types according to the conversion rate (Fig. 4b). The conversion rate of Y125F, Y365F, and Y541F declined remarkably, whereas those of Y122F, S138A, and E140V decreased at varying degrees. Compared with the wild type, the conversion rate of AD by each mutation was 1.44%^{Y125F}, 0.52%^{Y365F}, 2.52%^{Y541F}, 39.93%^{Y122F}, 23.64%^{S138A}, 38.99%^{E140V}, and 98.24%^{Y472F}. Thus, the activity of *KsdD* was almost abolished in Y125, Y365, and Y541. Meanwhile, Y122F, S138A, and E140V contributed differently to the activity of the enzyme, whereas Y472F did not affect enzyme activity.

Structural mechanism analysis of mutations

Pymol software (http://pymol.org/) was used to analyze the local structure of those mutations that aroused changes in *KsdD* activity. The hydroxyl group of Y365 was situated close to the C2 atom of the bound AD and served as the catalytic base that abstracted a proton from the C2 atom of AD (Fig. 5a). Y125 had no close contacts with the bound AD in the conformation of *KsdD* docking with AD, but its phenolic hydroxyl group was of hydrogen-bonding distance from the phenolic hydroxyl group of Y365 (Fig. 5b) and

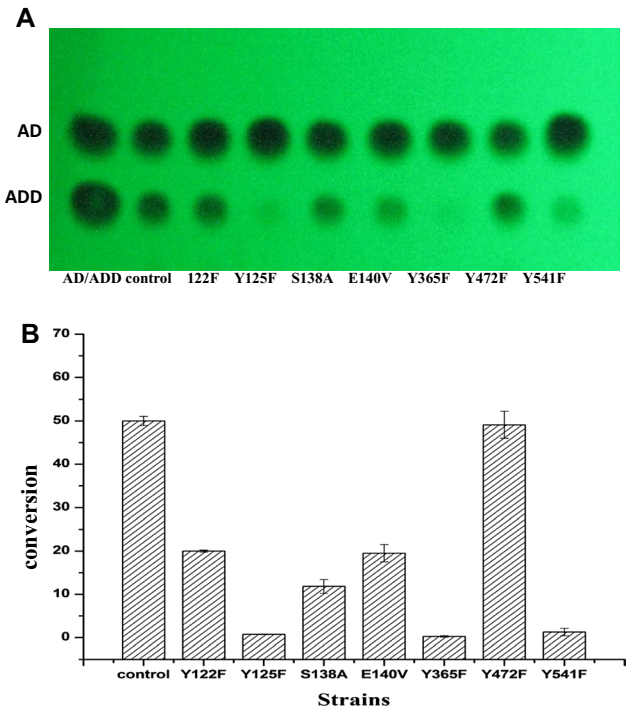

Fig. 4 AD conversion by mutation strains. **a** TLC analysis of AD conversion *Lane 1* standard AD and ADD; *lane 2 MNR; lane 3* Y122F; *lane 4* Y125F; *lane 5* S138A; *lane 6* E140V; *lane 7* Y365F; *lane 8* Y472F; *lane 9* Y541F. **b** HPLC analysis of AD conversion. *Lane 1 E. coli* BL21 (DE3)/pET-22b(+)-*KsdD-MNR; lane 2* Y122F; *lane 3* Y125F; *lane 4* S138A; *lane 5* E140V; *lane 6* Y365F; *lane 7* Y472F; *lane 8* Y541F

serve to increase the basic character of the catalytic base and facilitate proton relay.

In Fig. 6a, the distance between the hydroxyl group of Y541 and the C3 carbonyl oxygen of ADD was 3.5 Å. But

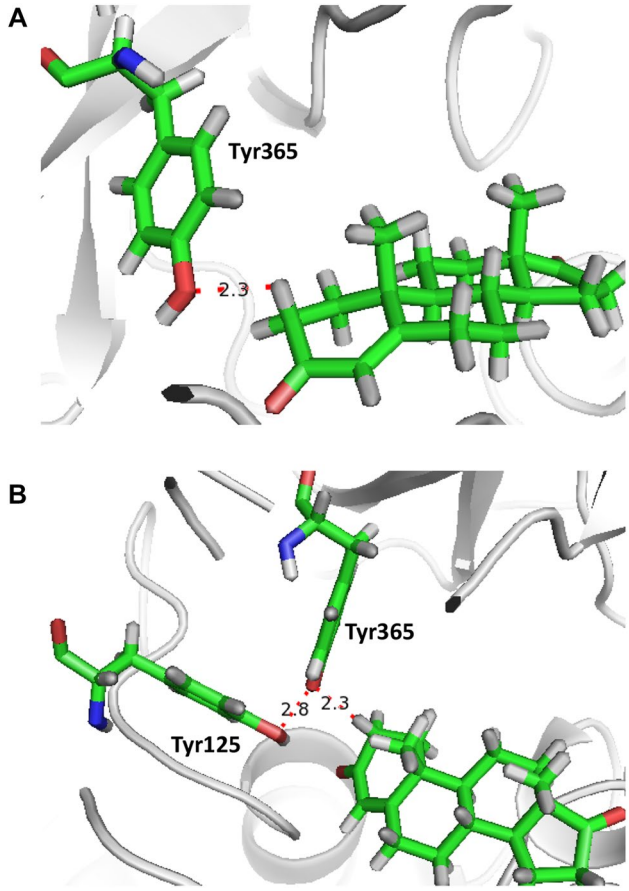

Fig. 5 Local model of the catalytic residues of *KsdD*-Tyr365 and Tyr125. **a** Local model of the catalytic residues of *KsdD*-Tyr365. **b** Local model of the catalytic residues of *KsdD*-Tyr125

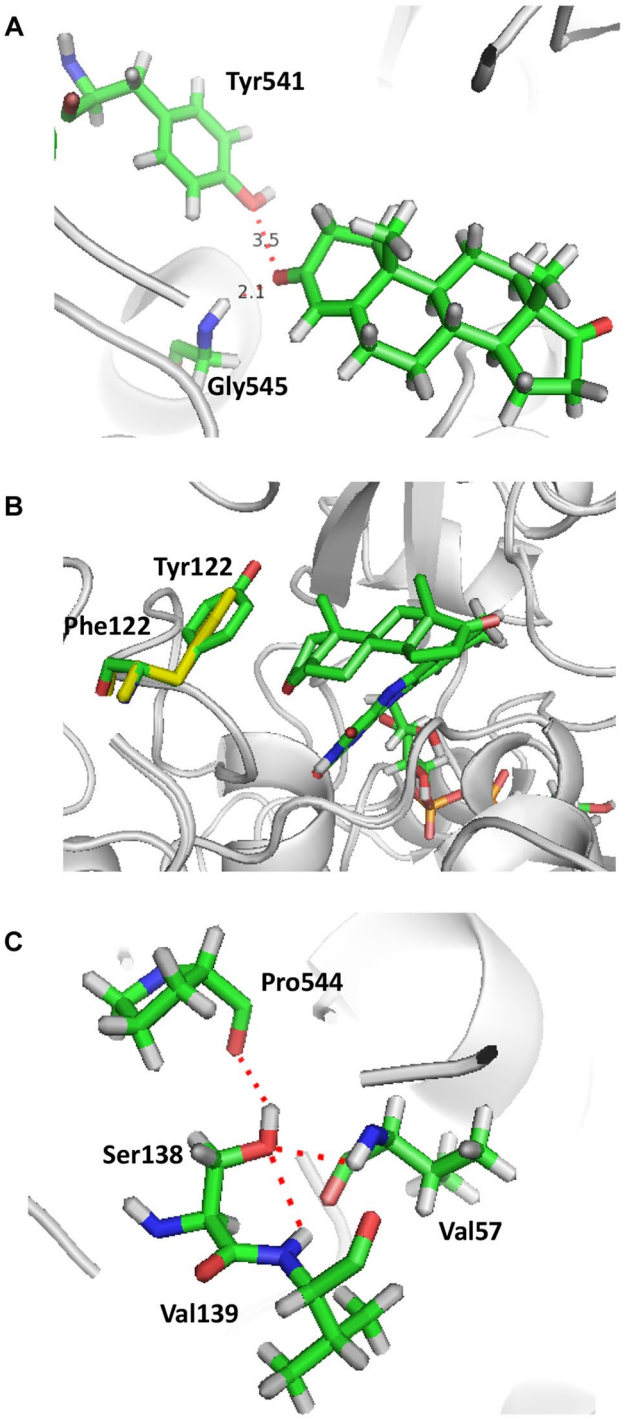

Fig. 6 Local model of the catalytic residues of *KsdD*-Tyr541/Tyr122/Ser138. **a** Local model of the catalytic residues of *KsdD*-Tyr541. **b** Superposition of residues Tyr122 and simulation of point mutations Phe122. **c** Local model of the catalytic residues of *KsdD*-Ser138

the Y541F mutation only showed a modest decline compared with Y365F and Y125F (Fig. 4b). This observation could be attributed to the backbone amide of G545, which within hydrogen bonding distance with the C3 carbonyl oxygen, together with Y541 to promote keto-enol tautomerization and labilization of the C2 hydrogen atoms.

The binding of AD molecule in the active site need a large number of van der Waals interactions (Rohman et al. 2013). As shown in Fig. 6b, Y122 is in a good position for hydrophobic stacking interactions with the B-ring of the 3-ketosteroid. This interaction is important for the binding of the steroid substrates(Matsushita and Itagaki 1992; Rohman et al. 2013). However, Y122F changed this position of Y122, which is detrimental to the binding of AD.

S138 located in the loop and in the hydrogen-bonding distance from V57, V139, and P544 (Fig. 6c). S138A and spontaneous mutation S138L (Xie et al. 2015) removed all the H bonds of S138, which could fix the movable loops. These loops may have a function in catalysis by shielding the FAD and substrate from the solvent (Oosterwijk et al. 2012).

In many flavoproteins, catalysis takes place at a location shielded from the solvent, which enhances the strength of polar interactions and is instrumental to substrate activation (Fraaije and Mattevi 2000; Mattevi 1998). E140

collaborated with five-membered D-ring of the 3-ketosteroid occupied a solvent-accessible pocket near the active site entrance (Fig. 7a). Shielded from the solvent to form hydrophobic platforms, which are important for substrate binding (Oosterwijk et al. 2012; Rohman et al. 2013).

The substrate conversion of Y472F showed no significant differences from the wild type. Given that the long distance between the sites of Y472 and substrate and the mutation of Y472F did not initiate hydrogen bond changes, Y472 may have no contribution to the catalysis of *KsdD*.

Discussion

Site-directed mutagenesis is an effective tool to improve certain biochemical or catalytic properties of proteins and is being widely used in the molecular modifications of industrial enzymes (Li et al. 2014; Seo et al. 2013). While the key issue is that which basic residues should be considered for mutation. The most important for the site-directed mutagenesis is the selection of mutation sites, and structure analysis can provide useful information in this aspect (Yang et al. 2013). *KsdD* is generally accepted as a membrane protein (Molnar et al. 1995; Plesiat et al. 1991; Wei et al. 2010). In addition, many attempts have been made to get the crystal of *KsdD* from *MNR* in our group. But as reports, the progress of expression (Shao et al. 2017) purification (Forneris et al. 2009) and crystallization (Rohman et al. 2012) of *KsdD* is tedious. Considering that, site-directed mutagenesis under the direction of in-silico protein docking modeling *KsdD* from *MNR* could provide a driection in the engineering of *KsdD* from *Mycobacterium*.

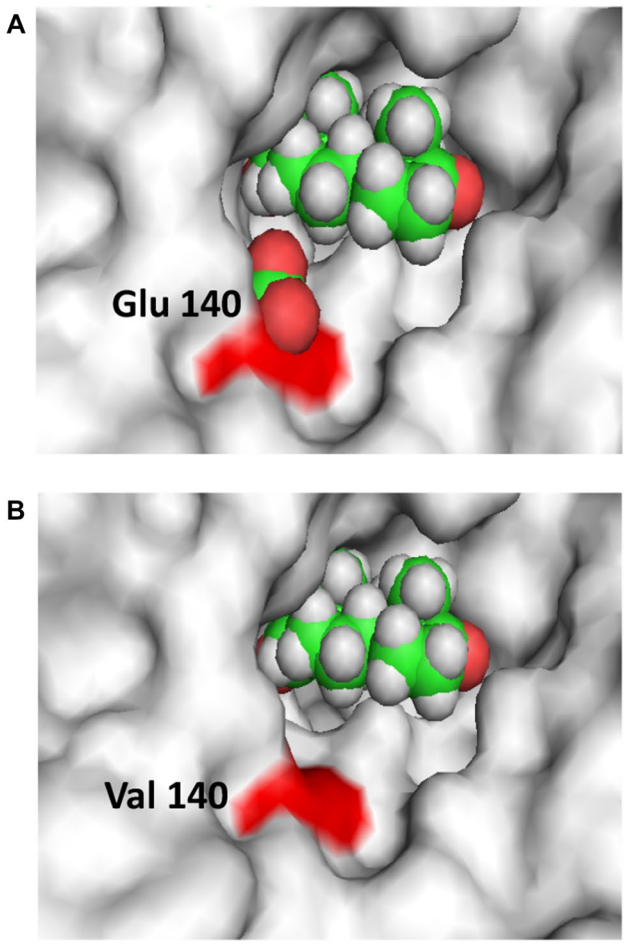

Fig. 7 Local model of the catalytic residues of *KsdD*-Glu140 and simulation of point mutations Va140. **a** Local model of the catalytic residues of *KsdD*-Glu140. **b** Simulation of point mutations Val140

The decline of the conversion of AD illustrated that Y125, Y365, and Y541 were essential to the function of *KsdD*. Y122, S138, and E140 contributed to the catalysis of *KsdD*. This indicated these residues could be potential sites to mutate in the engineering of *KsdD*. By combining the two-step mechanism of *KsdD* and the local structure, the mechanism of these amino acids could be explained.

The wild-type *KsdD* could introduce a double bond and then catalyze the ring-opening reaction of steroids. During this process, a concerted bimolecular elimination (E2) mechanism, in which the two hydrogens depart simultaneously without the formation of any intermediate, was considered less likely. In this study, we referred to the mechanism reported by Oosterwijk et al. (2012). Enzyme-catalyzed dehydrogenation likely followed a stepwise unimolecular elimination conjugate base (E1cB) mechanism, which was initiated by the interaction of the C3 carbonyl group of the 3-ketosteroid substrate with Y541 and G545 as an electrophile to promote labilization of the C2 hydrogen atoms. Subsequent abstraction of a proton from the C2 atom by Y365, which was assisted by Y125 as a general base, was proposed to result in either an enolate or a carbanionic intermediate; subsequently, a double bond was formed between the C1 and C2 atoms in synchrony with hydride transfer from the C1 atom of the substrate to the flavin coenzyme (Itagaki et al. 1990; Jerussi and Ringold 1965; Ringold et al. 1963). This process formed the indirect mechanism of Y122. In particular, the active site residues Y541 and G545 may act in tandem, so the absence of Y541 did not completely abolish the dehydrogenase activity of *KsdD*. Together, they promote keto-enol tautomerization and labilization of the C2 hydrogen atoms.

In addition, the hydroxyl groups of Y365 and Y541 of *KsdD* from *MNR* are in very similar positions to those of S468 and Y466 of Δ^4-(5α)-*KsdD*, respectively. Whereas in Δ^4-(5α)-*KsdD*, the S468 hydroxyl group abstracts a proton from the C4 carbon atom of the substrate, and in *KsdD* from *MNR*, the Y365 hydroxyl group is in a position to abstract a proton from C2. Finally, Y541 of *KsdD*

from *MNR* can promote keto-enol tautomerization at C3 keto-group, similar to Tyr466 of Δ^4-(5α)-*KsdD*.

In silico protein docking modeling showed that E140 was only 4 Å away from AD. This distance indicated that the carboxyl of Glu possibly reacted with the substrate. Although the conversion of AD decreased, the local structure of E140V showed that no H bonds were removed (Fig. 7b). Moreover, the mutation did not influence the key amino acid sites which as the general base to removed H of C2 of steroids. As shown in Fig. 7a, the residue E140 possibly maintained the hydrophobic environment of the active center.

In our previous study, we found that S138 of the *KsdD* of *MNR*, which spontaneously mutated to L138 of the *KsdD* of *MNR* M3, triggered the decline in *KsdD* activity (Xie et al. 2015). Furthermore, S138L was found to influence the stabilization of the loop. Considering the lack of the structure information of *KsdD* from *MNR*, the function of 138-amino acid was predicted to combine the crystal structure of the *KsdD* from *R. erythropolis* SQ1 and *KsdD*4 from *R. jostii* RHA1. For the C1,2-dehydrogenation reaction, we recognized that the fatty acid side chain of Leu may prevent the hydrophobic formation of the active center because of steric hindrance. In this study, in silico protein docking modeling revealed that AD in the loop, S138A, and S138L could remove the H bonds with V57, V139, and P544. Similar to the spontaneous mutations, the conversion of the substrate of S138A with the methyl side chain of Ala compared to S138L with iso-butyl side chain of Leu which has a higher steric hindrance declined, too. This phenomenon proved that these H bonds were essential for the activity of S138.

The catalytic function of *KsdD* was also partly clarified by docking screening and biotransformation assay. These results enabled us to identify the roles of the amino acid residues involved in catalysis, which will be useful in manipulating the catalytic properties of the enzyme and improving them for application in the pharmaceutical steroid industry. Nevertheless, in view of the importance of *KsdD* enzymes for industrial use, *KsdD* from *MNR* needs further investigation. With this information, we could establish a possible relationship between steroid and *KsdD* and clarify the reaction mechanisms of the enzyme. Therefore, future research should focus on the purification and structural characterization of *KsdD*.

Acknowledgements This work was supported by National Natural Science Foundation of China (21276196, 21406167), Key Project of Chinese Ministry of Education (213004A), and Tianjin Programs for Science and Technology Development (15ZCZDSY00510).

References

Adham NZ, Ei-Hady AA, Naim N (2003) Biochemical studies on the microbial Δ^1-dehydrogenation of cortisol by *Pseudomonas fluorescens*. Process Biochem 38(6):897–902

Bragin EY, Shtratnikova VY, Dovbnya DV, Schelkunov MI, Pekov YA, Malakho SG, Egorova OV, Ivashina TV, Sokolov SL, Ashapkin VV, Donova MV (2013) Comparative analysis of genes encoding key steroid core oxidation enzymes in fast-growing *Mycobacterium* spp strains. J Steroid Biochem Mol Biol 138:41–53

Donova MV (2007) Transformation of steroids by actinobacteria: a review. Appl Biochem Microbiol 43(1):1–14

Fernandes P, Cruz A, Angelova B, Pinheiro HM, Cabral JMS (2003) Microbial conversion of steroid compounds: recent developments. Enzyme Microb Technol 32(6):688–705

Fokina VV, Karpov AV, Sidorov IA, Andrjushina VA, Arinbasarova AY (1997) The influence of β-cyclodextrin on the kinetics of 1-en-dehydrogenation of 6α-methylhydrocortisone by *Arthrobacter globiformis* cells. Appl Microbiol Biotechnol 47(6):645–649

Forneris F, Orru R, Bonivento D, Chiarelli LR, Mattevi A (2009) Thermo FAD, a Thermofluor®-adapted flavin ad hoc detection system for protein folding and ligand binding. FEBS J 276(10):2833–2840

Fraaije MW, Mattevi A (2000) Flavoenzymes: diverse catalysts with recurrent features. Trends Biochem Sci 25(3):126–132

Fujii C, Morii S, Kadode M, Sawamoto S, Iwami M, Itagaki E (1999) Essential tyrosine residues in 3-ketosteroid-Δ1-dehydrogenase from *Rhodococcus rhodochrous*. J Biol 126(4):662–667

Geize RVD, Hessels GI, Gerwen RV, Vrijbloed JW, Meijden PVD, Dijkhuizen L (2000) Targeted disruption of the KstD gene encoding a 3-ketosteroid-delta(1)-dehydrogenase isoenzyme of *Rhodococcus erythropolis* strain SQ1. Appl Environ Microbiol 66(5):2029–2036

Geize RVD, Hessels GI, Gerwen RV, Meijden PVD, Dijkhuizen L (2001) Unmarked gene deletion mutagenesis of kstD, encoding 3-ketosteroid-Δ^1-dehydrogenase, in *Rhodococcus erythropolis* SQ1 using sacB as counter-selectable marker. FEMS Microbiol Lett 205(2):197–202

Geize RVD, Hessels GI, Dijkhuizen L (2002) Molecular and functional characterization of the KstD2 gene of *Rhodococcus erythropolis* SQ1 encoding a second 3-ketosteroid-Δ^1-dehydrogenase isoenzyme. Microbiology 148(10):3285–3292

Geize RVD, Yam K, Heuser T, Wilbrink MH, Hara H, Anderton MC, Sim E, Dijkhuizen L, Davies JE, Mohn WW, Eltis LD (2007) A gene cluster encoding cholesterol catabolism in a soil actinomycete provides insight into *Mycobacterium tuberculosis* survival in macrophages. Proc Natl Acad Sci USA 104(6):1947–1952

Itagaki E, Matushita H, Hatta T (1990) Steroid transhydrogenase activity of 3-Ketosteroid-Δ^1-Dehydrogenase from *Nocardia corallina*. J Biol 108(1):122–127

Jerussi R, Ringold HJ (1965) The mechanism of the bacterial C1, 2 dehydrogenation of steroids. III. Kinetics and isotope effects. Biochemistry 4(10):2113–2126

Li JF, Wei XH, Tang CD, Wang JQ, Zhao M, Pang QF, Wu MC (2014) Directed modification of the *Aspergillus usamii* β-mannanase to improve its substrate affinity by in silico design and site-directed mutagenesis. J Ind Microbiol Biotechnol 41(4):693–700

Liu C, Zhang X, Rao ZM, Shao ML, Zhang LL, Wu D, Xu ZH, Li H (2015) Mutation breeding of high 4-androstene-3,17-dione-producing *Mycobacterium neoaurum* ZADF-4 by atmospheric and room temperature plasma treatment. J Zhejiang Univ Sci B 16(4):286–295

Malaviya A, Gomes J (2008) Androstenedione production by biotransformation of phytosterols. Bioresour Technol 99(15):6725–6737

Marsheck WJ, Kraychy S, Muir RD (1972) Microbial degradation of sterols. Appl Microbiol 23(1):72–77

Matsushita H, Itagaki E (1992) Essential histidine residue in 3-ketosteroid-Δ^1-dehydrogenase. J Biochem 111(5):594–599

Mattevi A (1998) The PHBH fold: not only flavoenzymes. Biophys Chem 70(3):217–222

Molnar I, Choi KP, Yamashita M, Murooka Y (1995) Molecular cloning, expression in *Streptomyces livdans*, and analysis of a gene cluster from *Arthrobacter simplex* encoding 3-ketosteroid-Δ^1-dehydrogenase, 3-ketosteroid-Δ^5-isomerase and a hypothetical regulatory protein. Mol Microbiol 15(5):895–905

Oosterwijk N, Knol J, Dijkhuizen L, Geize RVD, Dijkstra BW (2012) Structure and catalytic mechanism of 3-ketosteroid-Δ^4-(5α)-dehydrogenase from *Rhodococcus jostii* RHA1 genome. J Biol Chem 287(37):30975–30983

Plesiat P, Grandguillot M, Harayama S, Vragar S, Michel-Briand Y (1991) Cloning, sequencing, and expression of the *Pseudomonas testosteroni* gene encoding 3-oxosteroid Δ1-dehydrogenase. J Biol 173(22):7219–7227

Ringold HJ, Hayano M, Stefanovic V (1963) Concerning the stereochemistry and mechanism of the bacterial C-1, 2 dehydrogenation of steroids. J Biol Chem 238(6):1960–1965

Rohman A, Oosterwijk NV, Dijkstra BW (2012) Purification, crystallization and preliminary X-ray crystallographic analysis of 3-ketosteroid-Δ^1-dehydrogenase from *Rhodococcus erythropolis* SQ1. Acta Crystallogr F 68(5):551–556

Rohman A, Oosterwijk NV, Thunnissen A-MWH, Dijkstra BW (2013) Crystal structure and site-directed mutagenesis of 3-ketosteroid-Δ^1-dehydrogenase from *Rhodococcus erythropolis* SQ1 explain its catalytic mechanism. J Biol Chem 288(49):35559–35568

Seo J, Ryu JY, Han J, Ahn JH, Sadowsky MJ, Hur H-G, Chong Y (2013) Amino acid substitutions in naphthalene dioxygenase from *Pseudomonas* sp. strain NCIB 9816-4 result in regio-and stereo-specific hydroxylation of flavanone and isoflavanone. Appl Microbiol Biotechnol 97(2):693–704

Shao ML, Zhang X, Rao ZM, Xu MJ, Yang TW, Li H, Xu ZH, Yang ST (2016) A mutant form of 3-ketosteroid-Δ^1-dehydrogenase gives altered androst-1, 4-diene-3, 17-dione/androst-4-ene-3, 17-dione molar ratios in steroid biotransformations by *Mycobacterium neoaurum* ST-095. J Ind Microbiol Biotechnol 43(5):691–701

Shao ML, Chen YL, Zhang X, Rao ZM, Xu MJ, Yang TW, Li H, Xu ZH, Yang ST (2017) Enhanced intracellular soluble production of 3-ketosteroid-Δ^1-dehydrogenase from *Mycobacterium neoaurum* in *Escherichia coli* and its application in the androst-1,4-diene-3,17-dione production. J Chem Technol Biotechnol 92(2):350–357

Shen YB, Wang M, Li HN, Wang YB, Luo JM (2012) Influence of hydroxypropyl-β-cyclodextrin on phytosterol biotransformation by different strains of *Mycobacterium neoaurum*. J Ind Microbiol Biotechnol 39(9):1253–1259

Shtratnikova VY, Bragin EY, Dovbnya DV, Pekov YA, Schelkunov MI, Strizhov N, Ivashina TV, Ashapkin VV, Donova MV (2014) Complete genome sequence of sterol-transforming *Mycobacterium neoaurum* strain VKM Ac-1815D. Genome Announc 2(1):e01177–13

Szentirmai A (1990) Microbial physiology of sidechain degradation of sterols. J Ind Microbiol 6(2):101–115

Wei W, Wang FQ, Fan SY, Wei DZ (2010) Inactivation and augmentation of the primary 3-ketosteroid-Δ^1-dehydrogenase in *Mycobacterium neoaurum* NwIB-01: biotransformation of soybean phytosterols to 4-androstene-3, 17-dione or 1, 4-androstadiene-3, 17-dione. Appl Environ Microbiol 76(13):4578–4582

Wovcha MG, Brooks KE, Kominek LA (1979) Evidence for two steroid 1,2-dehydrogenase activities in *Mycobacterium fortuitum*. Biochim Biophys Acta 574(3):471–479

Xie RL, Shen YB, Qin N, Wang YB, Su LQ, Wang M (2015) Genetic differences in KsdD influence on the ADD/AD ratio of *Mycobacterium neoaurum*. J Ind Microbiol Biotechnol 42(4):507–513

Yang HQ, Liu L, Shin HD, Chen RR, Li JH, Du GC, Chen J (2013) Structure-based engineering of histidine residues in the catalytic domain of α-amylase from *Bacillus subtilis* for improved protein stability and catalytic efficiency under acidic conditions. J Biotechnol 164(1):59–66

YuKimatsu K, Kaji A (1979) Preparation of androsta-3,17-diones. Japanese Patent 54,067,096

Zhang WQ, Shao ML, Rao ZM, Xu MJ, Zhang X, Yang TW, Li H, Xu ZH (2013) Bioconversion of 4-androstene-3, 17-dione to androst-1, 4-diene-3, 17-dione by recombinant *Bacillus subtilis* expressing KsdD gene encoding 3-ketosteroid-Δ^1-dehydrogenase from *Mycobacterium neoaurum* JC-12. J Steroid Biochem 135:36–42

Zhang QY, Ren Y, He JZ, Cheng SJ, Yuan JD, Ge FL, Li W, Zhang Y, Xie GR (2015) Multiplicity of 3-ketosteroid-Δ1-dehydrogenase enzymes in *Gordonia neofelifaecis* NRRL B-59395 with preferences for different steroids. Ann Microbiol 65(4):1961–1971

Zhong CS, Rao ZM, Xia HF, Xu ZH, Fang HY, Zhu GJ (2009) Mutation breeding of *Mycobacterium* sp. for transformation of phytosterol into androst-1,4-diene-3,17-dione. Chem Bioeng 7(3):43–46 (**in Chinese**)